

Characterization of a Residential Fire Sprinkler Using Phase Doppler Interferometry

John E. Widmann

U.S. DEPARTMENT OF COMMERCE
Technology Administration
Fire Safety Engineering Division
Building and Fire Research Laboratory
National Institute of Standards
and Technology
Gaithersburg, MD 20899



NIST

National Institute of
Standards and Technology
Technology Administration
U.S. Department of Commerce

Characterization of a Residential Fire Sprinkler Using Phase Doppler Interferometry

John F. Widmann

U.S. DEPARTMENT OF COMMERCE
Technology Administration
Fire Safety Engineering Division
Building and Fire Research Laboratory
National Institute of Standards
and Technology
Gaithersburg, MD 20899

August 2000



U.S. DEPARTMENT OF COMMERCE
Norman Y. Mineta, Secretary

TECHNOLOGY ADMINISTRATION
Dr. Cheryl L. Shavers, Under Secretary
of Commerce for Technology

NATIONAL INSTITUTE OF STANDARDS
AND TECHNOLOGY
Raymond G. Kammer, Director

CONTENTS

	<u>page</u>
1. Nomenclature	iii
2. List of Figures	iv
3. Abstract	1
4. Introduction	1
5. Experimental	3
6. Results and Discussion	4
7. Conclusion	13
8. Acknowledgements	14
9. References	15
10. Tables	18
11. Figures	20

NOMENCLATURE

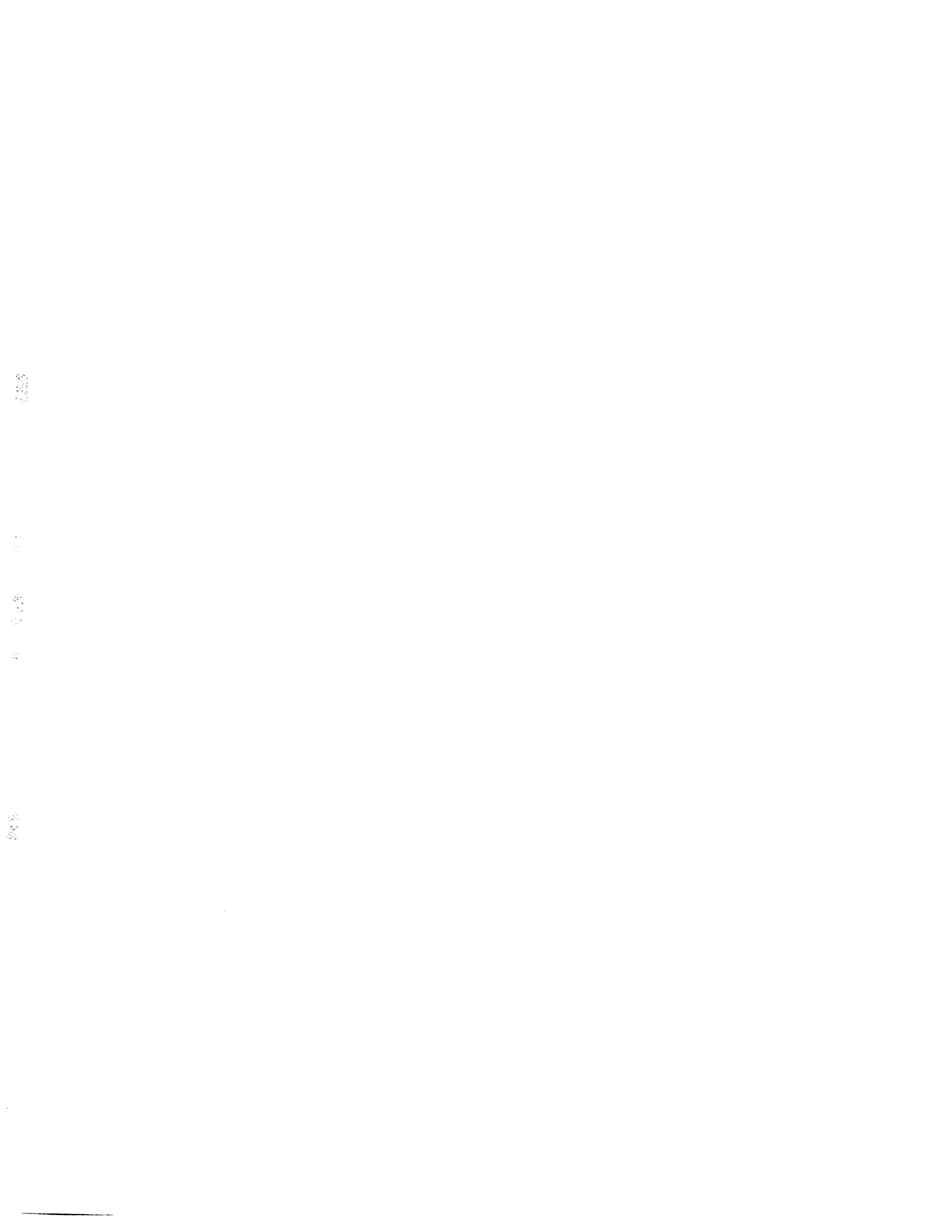
D_{10}	arithmetic mean diameter
D_{50}	volume mean diameter
D_{32}	Sauter mean diameter
f	sampling frequency
F	volume flux
k	coverage factor
K	sprinkler K-factor
N	number of replicated samples
N_d	drop number density
P	pressure
r	radial coordinate
s	standard deviation of replicated samples
s^2	variance of replicated samples
s_A, s_B	Type A and Type B uncertainties
U_c	combined standard uncertainty
v	velocity
v_z	axial velocity
v_r	radial velocity
V	volumetric flow rate

Greek Symbols

δ	fringe spacing
Δ_v	velocity resolution
λ	wavelength, nm
e	angular coordinate

LIST OF FIGURES

	<u>page</u>
Fig. 1 Schematic of the experimental facility.	20
Fig. 2 Photograph of the (A) experimental facility and the (B) residential sprinkler used in this study.	21
Fig. 3 Representative size distributions obtained with the PDI system at locations (A) near and (B) far from the fire sprinkler axis.	22
Fig. 4 The arithmetic mean diameter (D_{10}), volume mean diameter (D_{30}), and Sauter mean diameter (D_{32}) as a function of the radial coordinate in the spray.	23
Fig. 5 The mean axial and radial drop velocities measured in the spray as a function of the radial coordinate.	24
Fig. 6 The volume flux measured with the PDI system as a function of the radial coordinate.	25
Fig. 7 The measured number density as a function of the radial coordinate.	26
Fig. 8 The effect of the probe volume correction on the arithmetic mean diameter, D_{10} .	27
Fig. 9 The effect of the probe volume correction on the volume mean diameter, D_{30} .	28
Fig. 10 The effect of the probe volume correction on the Sauter mean diameter, D_{32} .	29
Fig. 11 Comparison of the volume flux measured with the PDI system and the pan test measurements.	30
Fig. 12 Oscilloscope traces showing the effect of burst splitting on the gate signal and the Doppler signal. The operating conditions correspond to (A) mixer frequency = 36 MHz, sample frequency = 40 MHz, and low pass filter = 20 MHz, and (B) mixer frequency = 40 MHz, sample frequency = 10 MHz, and low pass filter = 1.25MHz.	31
Fig. 13 The measured probe area as a function of the radial coordinate.	32



Characterization of a Residential Fire Sprinkler using Phase Doppler Interferometry

John F. Widmann *

Building and Fire Research Laboratory
National Institute of Standards and Technology
Gaithersburg, Maryland 20899-8640 USA

ABSTRACT

The results of a feasibility study to determine if the water sprays produced by residential fire sprinklers can be accurately characterized using phase Doppler interferometry (PDI) are presented. The large size of the water drops produced by fire sprinklers, and the relatively large coverage area of the spray, present significant challenges when attempting to characterize these sprays. These difficulties are especially relevant when using PDI because large drops and large coverage areas may result in trajectory dependent scattering errors and attenuation of the transmitting laser beams. For the residential sprinkler investigated, it was determined that trajectory ambiguity was not a significant source of error, but attenuation of the laser beam resulted in over-counting of drops due to burst splitting. This effect was minimized by properly choosing the operating conditions of the PDI processing electronics. For the spray investigated, the Sauter mean diameter varied from approximately 360 μm to 560 μm . Integration of the radial profile of the volume flux resulted in a calculated flow rate that agreed with the flow through the sprinkler to within 8 %. The results of this study demonstrate that PDI can be used to accurately characterize the sprays produced by residential fire sprinklers.

INTRODUCTION

The fire sprinkler is the most commonly used fire protection system, and it has been reported that the average fire loss in properties protected by sprinklers is about 10 % of that in non-protected properties [1]. The basic function of a fire sprinkler is to extinguish or control an accidental fire, and at the same time, to accomplish this with the least amount of water damage to the property. The effectiveness of the sprinkler spray at controlling a fire is governed by the spray characteristics (e.g., drop size, drop velocity, mass flux). For example, large drops can penetrate a rising fire plume to reach the fire source and wet combustible materials adjacent to the fire, whereas smaller drops will be entrained in the buoyant plume and carried away from the fire. Furthermore, the evaporating smaller **drops** have a cooling effect on the hot gases, and can prevent additional fire sprinklers from activating. It is therefore important that the spray

* e-mail: john.widmann@nist.gov

characteristics of fire sprinklers be understood if effective fire protection strategies are to be developed. The interested reader is referred to the recent review by Grant *et al.* [2] for a thorough discussion of fire suppression by water sprays.

The current rapid increase in computer technology has permitted increasingly more sophisticated modeling of the dynamics of fires. In particular, it is now possible to include the effect of water sprays on the fire spread, and to account for the complex interaction of this multiphase combustion process. For example, the Fire Dynamics Simulator (FDS) developed at the National Institute of Standards and Technology (NIST) is used to predict large scale fire phenomena [3, 4] in a variety of fire scenarios. However, to include the effect of fire sprinklers on the fire dynamics it is necessary to provide characteristics of the water spray produced by the sprinklers. This information is generally not available from the manufacturer, and must be experimentally determined.

Previous studies characterizing fire sprinkler sprays have utilized photographic techniques [5-8] and a laser-light shadowing method [9-12]. The photographic methods included illuminating the drops using strobe lighting and pulsed lasers, and using still photographs and video cameras for image capture. The laser-light shadowing technique utilized a modified commercially available instrument intended for cloud drop measurements. The drops were sized by determining the number of pixels shadowed as the drops passed through a visible laser-light sheet illuminating a linear photodiode array. The (one-dimensional) drop velocity was also determined by the length of time the pixels were shadowed.

More recently, Sheppard *et al.* [13] demonstrated that particle image velocimetry (PIV) can be used to measure droplet velocities in the sprays produced by residential fire sprinklers. Unfortunately, the PIV technique does not provide information on the droplet size distributions or size-velocity correlations. At the same conference, Gandhi and Stepan [14] presented PDI measurements in industrial fire sprinkler sprays. They compared their volume flux measurements with pan test measurements, in which the spray was collected in pans for a known period of time, resulting in an independent volume flux measurement. They reported that the comparison was poor when the pressure at the sprinkler head was 48.3 kPa-gauge (7 psig), but considerably better when the pressure at the sprinkler was 153.1 kPa-gauge (22.2 psig). The correlation coefficients were 0.5259 and 0.8912 for the former and latter cases, respectively. Presumably, the increase in pressure resulted in significant changes in the spray characteristics, likely shifting the size distributions towards the smaller drops. They also reported a correlation coefficient of 0.9993 when PDI volume flux measurements were compared with pan test measurements for a water mist nozzle. Size and velocity distributions were not presented; however, a plot showing the drop diameter versus time suggests that the data correspond to a bimodal size distribution. The authors did not report the uncertainty in the measurements, but the good agreement between the PDI volume flux measurements and the pan test measurements (for the sprinkler at 153.1 kPa-

gauge and the water mist nozzle) suggests that PDI may be a promising technique for characterizing fire sprinkler sprays. This paper presents the results from a feasibility study to evaluate the applicability of phase Doppler interferometry for characterizing water sprays produced by residential fire sprinklers.

EXPERIMENTAL

A sprinkler characterization facility has been constructed in the Building and Fire Research Laboratory at NIST for the purpose of characterizing residential and industrial fire sprinklers and water mist suppression systems. The facility, presented in Fig. 1, consists of an enclosed area equipped with the necessary piping and pumps to operate under a variety of flow conditions. The water is collected and recirculated back to the sprinkler, forming a closed loop system. The total dimensions of the enclosed pool used to collect the water spray is 6 m x 6 m, and the sprinkler can be mounted at one of several ports 1.6 m above the floor. A variety of diagnostics are being investigated for use in the facility to characterize the water sprays produced by fire sprinklers and mist generation systems.

The measurements presented here correspond to the spray generated from a 'Reliable' residential fire sprinkler (Model GFR QR 701A) with a K-factor of $1.35 \times 10^{-4} \text{ m}^3 \text{ s}^{-1} \text{ kPa}^{-0.5}$ ($5.6 \text{ gal min}^{-1} \text{ psig}^{-0.5}$). The pressure at the sprinkler head was maintained at $2.8 \text{ kPa} \pm 0.15 \text{ kPa}$ ($19 \text{ psig} \pm 1 \text{ psig}$), resulting in a flow rate through the sprinkler of $1.54 \times 10^{-3} \text{ m}^3 \text{ s}^{-1} \pm 0.051 \times 10^{-3} \text{ m}^3 \text{ s}^{-1}$ ($24.4 \text{ gpm} \pm 0.8 \text{ gpm}$). This sprinkler head, shown in Fig. 2, is a common fire sprinkler for residential applications, and was operated under a typical pressure. The sprays produced by fire sprinklers are large compared to systems in which PDI is typically applied, and cover an area on the order of 10 m^2 . Due to the large coverage area, it is necessary to locate the PDI transmitting and receiving optics directly in the spray. This was accomplished by encasing both the transmitting and receiving optical systems in water-tight containers equipped with a purge of dry air to prevent moisture from condensing on the optics. The PDI optics are mounted to a rectangular translation stage that can be moved in either horizontal direction. The measurements were obtained in a horizontal plane $1.12 \text{ m} \pm 0.01 \text{ m}$ below the sprinkler.

The experiments were conducted using a 2-component phase Doppler interferometer with a Real-time Signal Analyzer (RSA) available from TSI, Inc. A 300 mW air-cooled argon ion laser operating in multi-line mode was used as the illumination source, and the green ($\lambda = 514.5 \text{ nm}$) and blue ($\lambda = 488 \text{ nm}$) lines were used to measure the axial and radial velocity components, respectively. The transmitting optics were coupled to the beam conditioning optics using fiber optic cables, which permitted the transmitting optics

* Certain commercial equipment, materials, or software are identified in this manuscript to specify adequately the experimental procedure. Such identification does not imply recommendation or endorsement by the National Institute of Standards and Technology, nor does it imply that the materials or equipment are necessarily the best available for this purpose.

to be located in the spray. The front lens on the transmitting optics had a focal length of 1000 mm, and a 50 mm extender was used to increase the maximum measurable drop size to 950 μm . The receiving optics were located at a scattering angle, θ , of $33^\circ \pm 1^\circ$ measured from the direction of propagation of the laser beams. The relatively long focal lengths of the front lenses on the receiving and transmitting optics necessitate a relatively large translation stage, and limit how close the probe volume can be located to the walls of the enclosed area.

The PDI signal processor **was** initially operated with the settings recommended by the manufacturer for the flow investigated (mixer frequency = 36 MHz, sample frequency = 40 MHz, low pass filter = 20 MHz), although it was found that the system operated more effectively under other settings. This **was** due to burst splitting events that caused the processor to over-count drops, which is discussed further below. The processor settings used when collecting the data presented in this paper were: mixer frequency = 40 MHz, sample frequency = 10 MHz, low pass filter = 1.25 MHz. Hardware coincidence, which requires that drops be detected on both PDI channels simultaneously to be validated, was used **as** an additional validation criteria for all measurements. An intensity validation scheme was utilized to account for trajectory dependent scattering errors; however, the occurrence of such errors was found to be minimal.

RESULTS AND DISCUSSION

Spray Characterization

Phase Doppler interferometry measurements were obtained in the water spray produced by a residential fire sprinkler to assess the accuracy of the technique for characterizing such sprays. Figure 3 presents representative size distributions collected at two locations in the spray. In each case, three size distributions, corresponding to replicated measurements at the same location, are shown to demonstrate the variability in the runs. The size distributions presented in Fig. 3A and Fig. 3B corresponds to data collected close to and far from the sprinkler axis, respectively. In general, data collected close to the sprinkler produced size distributions represented reasonably well by a log-normal model. Data obtained farther from the sprinkler, which are more heavily weighted by larger drops, produced size distributions more accurately modeled by Rosin-Ramler size distributions. Current efforts in our laboratory include representing size distributions at all locations in the spray as a weighted mixture of log-normal and Rosin-Ramler distributions. Such a size distribution model could easily be incorporated into computational models intended to predict the interaction of fires and the water sprays produced by the experimentally characterized sprinklers.

Radial profiles of the arithmetic mean diameter (D_{10}), volume mean diameter (D_{30}), and Sauter mean diameter (D_{32}) are shown in Fig. 4. Here the customary notation of Mugele and Evans is used [15]. The profiles represent data averaged over various angular coordinates, θ . The spray data presented correspond to 370 samples collected at

120 locations in a horizontal plane $1.12 \text{ m} \pm 0.01 \text{ m}$ below the sprinkler head. A sample consisted of 2000 drop attempts. The actual number of drops measured was less than this because not all signals were validated. Collecting larger sample sizes was impractical due to the low data rates associated with this low number density spray. Data rates typically varied from 0.1 Hz to 10 Hz. The measured values of D_{10} , D_{30} , and D_{32} were not found to vary significantly with the angular coordinate, but increased with increasing radial coordinate as shown in the figure. The arithmetic mean diameter, D_{10} , varied from approximately $200 \text{ }\mu\text{m}$ where the size distributions were heavily weighted by the smaller drops to over $500 \text{ }\mu\text{m}$ in the outer region of the spray. For large values of the radial coordinate, r , the size distributions are dominated by larger drops because the smaller drops have insufficient initial momentum to reach the outer spray region. The error bars in Figs. 4 through 7 correspond to the combined standard uncertainty with a coverage factor of $k = 2$, or roughly a 95 % confidence interval [16, 17]. The quantification of the measurement uncertainty is discussed further below.

The mean values of the axial (positive values correspond to downward) and radial drop velocities are presented as a function of the radial coordinate in Fig. 5. As in Fig. 4, the data have been averaged over the angular coordinate. The drop velocities, like the characteristic sizes shown in Fig. 4, were not found to vary significantly with the angular coordinate. The mean axial velocity is relatively low near the sprinkler axis (inner region of the spray), but increases with the radial coordinate until a maximum value of approximately 2.5 m s^{-1} at $r = 100 \text{ cm}$ is reached. The radial coordinate at which the mean axial velocity reaches a plateau corresponds to the location where the characteristic sizes begin to increase with r . The mean radial component of the drop velocity ranges from roughly -0.25 m s^{-1} to 1.5 m s^{-1} , and also increases with radial coordinate. In the inner region of the spray, negative radial velocities indicate a recirculation zone produced by the momentum transfer between the spray and the ambient gas.

Volume flux measurements are presented in Fig. 6 revealing that most of the water spray at this horizontal plane (1.12 m below the sprinkler) flows through an annular ring approximately 0.5 m wide and centered at $r \approx 1.2 \text{ m}$. The angular variation in the volume flux measurements was greater than the size or velocity measurements, which is attributed to the presence of the yoke arms that hold the deflector plate in place, the grooves on the deflector plate, and the inherent uncertainty in PDI volume flux measurements. Although the volume flux measurements display greater variation with the angular coordinate than the size and velocity measurements, there is no obvious dependency on θ . This may be due to the randomness of the spray or insufficient measurement resolution. Although PDI is capable of measurements with fine resolution, the large coverage area of the sprinkler spray makes such measurements impractical. This is the primary disadvantage of using PDI in very large sprays like the one investigated here. Regardless of the cause, averaging over the angular coordinate, and including the angular variations in the Type A uncertainties as was done in Fig. 6, results

in useful volume flux profiles with reasonable measurement uncertainties, appropriate for use in fire dynamics models.

The volume flux profile shown in Fig. 6 can be integrated over the radial coordinate to obtain a flow rate through the measurement plane, which can be compared with the **flow** rate of water through the sprinkler. The volumetric flow rate, V , through the sprinkler can be determined from the K-factor and the pressure at the sprinkler head using the relation

$$V = KP^{0.5}, \quad (1)$$

Where K is the numerical K-factor in the appropriate units and P is the water pressure (gauge) at the sprinkler head. Applying Eq. (1) for the conditions used here, $V = 1.54 \times 10^{-3} \text{ m}^3 \text{ s}^{-1} \pm 0.051 \times 10^{-3} \text{ m}^3 \text{ s}^{-1}$. Integration of the volume flux profile in Fig. 6 results in a flow rate through the measurement plane of $1.43 \times 10^{-3} \text{ m}^3 \text{ s}^{-1} \pm 0.145 \times 10^{-3} \text{ m}^3 \text{ s}^{-1}$. Therefore, the integrated flow rate agrees with the value calculated from the sprinkler K-factor to within 8 %, indicating that the volume profiles presented in Fig. 6 are consistent with the total flow of water through the sprinkler head.

Using the data presented in Figs. 4 and 6, a mean volume diameter, \overline{D}_{30} , for the spray can be calculated from

$$\overline{D}_{30} = \frac{\int_0^{\infty} D_{30}(r)F(r)r \, dr}{\int_0^{\infty} F(r)r \, dr}, \quad (2)$$

where $F(r)$ is the volumetric flux at r . For the spray investigated here, $\overline{D}_{30} \approx 422 \text{ } \mu\text{m}$. This is a useful parameter for concisely quantifying the drop size of a sprinkler spray. Combined with the volume flux data, it can also be useful for preliminary modeling efforts to explore the interaction of the sprinkler spray with a fire. For example, the adequacy of submodels for drop transport and evaporation can be investigated for a drop size corresponding to the actual spray without introducing the complications associated with polydisperse spray systems.

The measured drop number density is presented in Fig. 7. The data reveal that this is a relatively low number density spray despite the large volumetric flow rate of water through the sprinkler. The number density is relatively uniform at approximately 6 cm^{-3} for $r < 1 \text{ m}$, and then decreases for increasing radial coordinate. There are two sets of error bars presented in the figure. The inner error bars correspond to the pooled Type A ($2s_A$) uncertainties [18] and indicate the variability as determined by replicated measurements. The outer error bars represent the combined standard uncertainty ($2[s_A^2 + s_B^2]^{1/2}$) and indicate the difficulty in accurately quantifying the number density using PDI in this spray. The relative uncertainty in the number density measurements is considerably larger than the measurements reported above, the cause of which will be discussed further below. Note that for the purposes of predicting fire suppression

effectiveness and providing inlet conditions for computational simulations, the parameters of primary interest are size, velocity, and volume flux. The number density profiles are of secondary importance for these applications. Therefore, the large uncertainty in the number density measurements does not represent a significant limitation in using PDI for fire sprinkler characterization.

Uncertainty Analysis

Because the objective of this work is to evaluate the feasibility of using phase Doppler interferometry to characterize residential fire sprinkler sprays, accurate assessment of the uncertainty in the measurements is of fundamental importance. Consequently, considerable effort **was** directed toward this goal. This section describes the methodology used to arrive at quantified uncertainties in the PDI measurements.

The PDI measures the size **and** velocity of individual drops as they pass through the sample volume. The uncertainties associated with the measurements of the drop size and velocity are related to the PDI optical and electronic systems, and are relatively easy to assess. Furthermore, these uncertainties are typically low. However, the size and velocity of individual drops are rarely of interest. Instead, it is usually the size and velocity *distributions* that are desired. Estimating the distributions introduces additional uncertainty due to effects like the size dependent probe volume and missed drops. Friedman and Renksibulut [19] recently presented a succinct overview of the various factors contributing to the uncertainties of PDI measurements. A noteworthy conclusion of their analysis is that due to the large uncertainties, and the difficulty in their quantification, volume flux measurements should be used in a qualitative fashion rather than quantitatively. Furthermore, we note that the same conclusion may be drawn concerning number density measurements obtained with PDI. When investigating fire sprinkler sprays with PDI, however, the uncertainty in the volume flux measurements can be quantified by comparison with pan test measurements.

The measurement uncertainties reported here reflect contributions from a statistical analysis of replicated measurements (Type A uncertainties), and those that are due to the instrument and can not be quantified using statistical methods (Type B uncertainties) [16, 17]. Calculating the Type A uncertainties requires only that multiple measurements be obtained at each location. Quantifying the Type B uncertainties, however, is considerably more difficult.

Drop Size

The uncertainty in PDI size measurements is essentially determined by the error in the slope **of** the diameter versus phase shift curve. This function describes the (linear) relation between the diameter of the measured drops and the phase shift between the high frequency Doppler signals measured on multiple detectors. This relationship has been discussed in detail by numerous researchers, and is the basis for the sizing capabilities of

PDI systems [20, 21]. Accounting for both the uncertainty in the scattering angle (1 %) and the uncertainty in the refractive index of the water drops due to possible contaminants (1 %), the total uncertainty in the size measurement is within 1.4 %. Here it has been assumed that errors introduced due to uncertainties in the detector spacing (which have been recently calibrated by the manufacturer) are negligible.

Drop Velocity

For the optical arrangement used in this study, the uncertainty in the velocity measurement of individual drops, v , is dominated by the method in which the processor bins the data. Individual velocity measurements are stored in one of 512 bins spanning the entire velocity range by the PDI processor. The width of these bins contributes to the uncertainty in the velocity measurements, and is determined by the fringe spacing and sampling frequency. Therefore, the velocity resolution, Δ_v , can be computed from

$$\Delta_v = \frac{1}{512} \frac{f}{\delta}, \quad (3)$$

where f is the sampling frequency, and δ is the fringe spacing [22]. Because fire sprinkler sprays produce relatively large drops, it is necessary to use large fringe spacings in the probe volume. For the optical configuration used here, the fringe spacings are 25.778 μm and 24.280 μm for the green and blue laser beams, respectively. The fringe spacing is determined by the wavelength of the laser beams and the beam intersection angle. For this system, the uncertainty in δ is negligible compared to the effect of binning the data. The data presented here were obtained using a sample frequency of 10 MHz. Therefore, Eq. (3) predicts measurement uncertainties of 0.504 m s^{-1} and 0.535 m s^{-1} for the axial and radial velocity components, respectively. The mean values of the Type B uncertainties are summarized in Table 1.

It is interesting to note that for the PDI configuration used here, the relative uncertainty in the velocity measurement is considerably greater than that of the size measurement. It is a common misconception that phase Doppler velocity measurements are necessarily more accurate than the corresponding size measurements. The Type B uncertainties presented in Table 1 illustrate that this is not necessarily the case, and that the respective uncertainties depend upon the configuration of the PDI system.

D_{10} , D_{30} , and D_{32}

As stated above, it is generally not the characteristics of individual drops that are of concern. Rather, one is usually interested in distributions or moments of the distributions. Here we have reported values of the arithmetic mean diameter, the volume mean diameter, and the Sauter mean diameter. There are considerably more sources of error in the size distribution measurements than the individual drop size measurements discussed above. Some of these include undetected drops, saturated signals, trajectory

ambiguity errors, invalidated drops, oscillations in the diameter versus phase shift curve, and the application of the probe volume correction. Details on these aspects of PDI can be found in references [19-27] and others.

By varying the photomultiplier tube (PMT) detector voltage and observing the effect on the low end of the size distributions, it was determined that the number of small drops being missed during the measurements was not significant. Because the value of D_{10} is heavily influenced by the smaller drops, a 2 % error in the value of D_{10} is assumed due to small drops that may have been missed. Missed drops are assumed to contribute negligible error into the calculated values of D_{30} and D_{32} because these parameters are weakly influenced by the smaller drops.

For the operating conditions used here, detector saturations were observed very rarely during the measurements. Furthermore, the error introduced due to saturated signals is likely to be negligible because the RSA processor used here effectively validates saturated signals. This is because the processor searches for zero-crossings in the high frequency Doppler signal, and the locations of the zero-crossings are not impacted by saturated signals. Therefore, saturated signals are assumed to introduce negligible error into the determination of D_{10} , D_{30} , and D_{32} .

Trajectory dependent scattering errors (also called trajectory ambiguity errors) are another possible source of uncertainty in the measurements; however, this was not found to be significant in the present study. An intensity validation method [22, 24, 26] was used to minimize such errors, but relatively few drops were rejected. It is assumed that trajectory ambiguity introduced negligible error in D_{10} , and contributed only 0.5 % uncertainty to the values of D_{30} and D_{32} . Oscillations in the diameter versus phase shift relation are not significant when investigating fire sprinkler sprays due to the large size of the drops, and this effect was neglected in the uncertainty estimates.

The validation fraction for velocity measurements was typically between 90 % and 95 %, with the validation for the sizing measurements somewhat lower (typically 50 % - 70 %). Invalidated signals can occur for many reasons, and the invalidated signals may not correspond to drops passing through the probe volume. It is interesting to note that the validation fractions were higher for the sizing measurements before the effect of burst splitting events on the data was minimized. In this case, attenuation of the transmitting laser beams resulted in Doppler signals being split into multiple “bursts”. The split bursts were being interpreted as multiple drops, which resulted in higher validation fractions [28]. The cause of burst splitting in PDI measurements is discussed below, and the manner in which the effect on the data was minimized is also presented. A thorough discussion of burst splitting events in PDI measurements is presented in reference [27]. The above illustrates that using the validation fraction to assess the quality of PDI measurements can be misleading. Invalidated signals will not affect the measured size distributions provided there is no size bias to the rejections, and it is not believed that any such bias occurred during the measurements reported here. Nonetheless, a relative

contribution of 1 % to the uncertainty in D_{10} , D_{30} , and D_{32} was assumed to account for any possible bias.

The probe volume correction (PVC), which removes the bias due to the size dependence of the probe area, is another possible source of uncertainty in the size distribution measurements. This was explored by determining the effect of the PVC on the calculated values of D_{10} , D_{30} , and D_{32} . Figure 8 shows the effect of the PVC on the calculated values of the arithmetic mean diameter. Note that for large values of D_{10} , the correction is only 2 % - 3 %. However, for small values of D_{10} , the PVC has a much greater effect. The solid line is a least-squares fit to the data of the form AD_{xy}^B , and represents a mean correction to D_{10} due to the PVC as a function of D_{10} . Similar plots are shown in Figs. 9 and 10 for the effect of the probe volume correction on D_{30} and D_{32} , respectively. The curves in Figs. 8, 9, and 10 show the effect of the PVC, not the error due to it. It is necessary to make an assumption as to the accuracy of the probe volume correction if this effect is to be included in the Type B uncertainty calculation. As a conservative estimate, the error introduced in the characteristic diameters (D_{10} , D_{30} , and D_{32}) due to the PVC is assumed to be 15 % of the correction shown in Figs. 8, 9, and 10. Therefore, the uncertainty due to the PVC is $(0.15)(3.4522 \times 10^6)D_{10}^{-3.1571}$, $(0.15)(3.8478 \times 10^{10})D_{30}^{-4.7049}$, and $(0.15)(2.1131 \times 10^{18})D_{32}^{-7.6043}$ for the calculated values of D_{10} , D_{30} , and D_{32} , respectively. The Type B uncertainties for D_{10} , D_{30} , and D_{32} are summarized in Table 1. Note that the entries in Table 1 for the probe volume correction were calculated assuming mean values of 350 μm , 400 μm , and 450 μm for D_{10} , D_{30} , and D_{32} , respectively.

The various sources of the Type B uncertainty discussed above were evaluated at each radial location and combined. The Type A uncertainties were also evaluated at each location as the standard error of the mean, $sN^{1/2}$, where s is the standard deviation of the data and N is the number of samples. The Type A and Type B uncertainties were combined by summing the respective variances, s_A^2 and s_B^2 , and these are presented in the figures.

Mean Velocity

As discussed above, the velocity resolution is only $\approx 0.5 \text{ m s}^{-1}$ for the PDI configuration used here. This represents a rather large relative uncertainty in the velocity measurement for individual drops. Fortunately, the uncertainty in the *mean* velocity is not limited by the discrete binning, as is the case for individual drop velocity measurements. The variance of the binned velocity data does, however, differ from the correct variance. This difference can be estimated, and the variance corrected, using Sheppard's correction for variance [29],

$$s_{corrected}^2 = s_{grouped}^2 - \frac{\Delta_v}{12}. \quad (4)$$

For the data presented here, this correction is small, and using the variance from the grouped data introduces little error. Furthermore, the best estimate for the true mean is the center of the bin in which the calculated mean velocity is located [29]. The calculated mean velocities, therefore, have considerably smaller uncertainties than the velocity measurements corresponding to individual drops.

Volume Flux

Figure 11 presents a comparison between the volume flux measurements obtained with the PDI system and pan test measurements in which the flux was measured using a graduated cylinder and a stopwatch. Note that although the measurement area for the pan tests ($31.4 \text{ cm}^2 \pm 1.0 \text{ cm}^2$) is considerably larger than that of the PDI measurements (of order 0.01 cm^2), it is orders of magnitude smaller than the area of the spray (approximately 10 m^2). Because the characteristics of the spray are not expected to vary significantly over the dimensions of the pan test measurement area, the fluxes determined from the pan tests can be compared directly with those obtained from the PDI measurements.

The filled symbols in Fig. 11 correspond to measurements taken using the recommended PDI operating conditions. It is evident that the measured volume **flux** is considerably higher than the actual flux, and also that there is considerable variation in the measurements. The vertical error bars represent only the Type A uncertainties (**2s**). The horizontal error bars represent the 6.6 % combined standard uncertainty, $2U_c$, of the pan test measurements. This uncertainty includes both Type A and Type B uncertainties, and therefore accounts for experimental errors not captured in the variance of the replicated measurements.

The PDI volume **flux** measurements are significantly higher than the actual flux due to the occurrence of burst splitting events. To measure the large drops present in this spray, it is necessary to use a lens with a large focal length on the transmitting optics. This provides the increased fringe spacing necessary to size large drops. Because the coverage area of the spray and the distance between the transmitting optics and the probe volume are both large, the probability is high that drops will pass through the transmitting laser beams while another drop is in the sample volume. The result of drops attenuating the transmitting beams is a momentary loss of the fringe pattern. The processor improperly interprets this as the drop leaving the sample volume, and when the fringe pattern reappears, it is interpreted as another drop entering the sample volume. The result is that single drops are erroneously counted as multiple drops. Furthermore, the transit time of the drop is calculated incorrectly, which affects the calculation of the probe area and probe volume correction. Thus, the burst splitting events have a significant impact on the data, particularly the volume flux, number density, and probe volume correction. Examples of oscilloscope traces of the gate signal and the measured Doppler signal are

shown in Fig. 12 for cases in which the split burst was measured as multiple drops (Fig. 12A) and as a single drop (Fig. 12B).

The open symbols in Fig. 11 correspond to PDI volume flux measurements obtained with the operating conditions optimized to minimize the effect of burst splitting. Note the much better agreement between the PDI volume flux measurements and the pan test measurements. To minimize the impact that burst splitting events have on the measurement, the sample frequency was reduced from 40 MHz to 10 MHz. This is the lowest value of the sample frequency used because attempts to calibrate the detector phase shifts at lower frequencies were unsuccessful. The cause of the unsuccessful calibrations is unknown and is under investigation.

The reason that the impact of the burst splitting events on the measurements is minimized by lowering the sampling rate is related to the discreteness of the sampling process used during PDI measurements. Reducing the sampling frequency has a beneficial effect on the measurements because the periods of low intensity that cause the bursts to be split are short-lived. By reducing the sampling rate, the probability that the processor will sample through the splitting event without detecting the brief periods of low signal intensity (below the signal threshold) is increased. As a result, the processor does not “close” the gate, which would falsely indicate that the drop has left the probe volume.

To operate the PDI at lower sampling rates, it is necessary to change the mixer frequency from 36 MHz to 40 MHz. This is because the acousto-optic modulator (also called a Bragg cell) imparts a false velocity corresponding to a frequency of 40 MHz on the measurements. Using a mixer frequency of 36 MHz results in this bias frequency being reduced to 4 MHz. However, to operate the PDI at low sampling frequencies, it is necessary to eliminate this bias by using a mixer frequency of 40 MHz. It should be noted that reducing the frequency in this manner is feasible because of the relatively low drop velocities encountered in fire sprinkler sprays. The sprinkler investigated here produced drops with axial and radial velocity components below 3 m s^{-1} at the elevation examined (approximately one meter below the sprinkler head). When investigating high speed flows, it may be impractical to reduce the sample frequency in the manner done here. The impact of burst splitting events on the data has been extensively investigated, and those results are presented elsewhere [28]. Burst splitting events have also been reported previously by Lazaro [30] and Van Den Moortel *et al.* [31].

Using the data presented in Fig. 10, it was determined that the mean relative error in the volume flux measurement is approximately 20.3%. Furthermore, it was found that the dominant source of measurement uncertainty is the uncertainty in the probe area calculation, and that the mean relative error in the volume flux can be reduced to 14.0% by applying a post-processing correction in which an improved estimate of the probe area is used. This correction involves utilizing data from multiple sample runs obtained under the same conditions, and is described elsewhere [32]. It should be noted that improving

PDI volume **flux** measurements is currently an active research area (e.g., [33]) and such improvements would translate to improved capabilities for fire sprinkler characterization.

Probe Area

The calculated probe area is presented in Fig. 13 as a function of the radial coordinate, where the error bars correspond to the combined standard uncertainty ($k = 2$). The Type B uncertainty was determined to be 0.0010 cm^2 for the measurements presented here [32]. The Type A uncertainty decreases with radial coordinate, which is attributed to the size distribution shifting towards the larger drops for increasing values of r . The probe area used in the volume flux calculation corresponds to the largest drops in the distribution. The counts in the bins associated with the smaller drops are then corrected to account for the size dependence of the probe area. Thus, the sampling statistics are improved for measurements in which there are many drops in the larger size classes.

Number Density

Of the measurements reported here, the uncertainty in the number density is the most difficult to quantify. The same factors that contribute to the uncertainty in the volume **flux** measurement will also contribute to the uncertainty in the number density measurement. Furthermore, if small drops are not detected, it will have a negligible impact on the volume **flux** measurement but will have a greater effect on the measured number density. For this reason, the relative uncertainty (Type B) in the number density measurements was assumed to be 1.5 times that of the volume flux measurements. The difficulty quantifying the measurement uncertainty should be taken into consideration if quantitative number density measurements are desired.

Table 2 summarizes the mean relative uncertainties in the measurements ($2U_c$). As discussed above, the uncertainties depend upon the value of the measured parameter. For example, the uncertainty in D_{10} decreases as D_{10} increases. This dependence is not included in Table 2, rather the values presented represent the ratio of the mean uncertainty to the mean value of the measured parameter (e.g., $\overline{A \& B}$, where the overbar indicates a mean quantity).

CONCLUSION

The applicability of phase Doppler interferometry (PDI) was evaluated for characterizing the water sprays produced by residential fire sprinklers. Reported measurements include volume flux, number density, arithmetic mean diameter (D_{10}), volume mean diameter (D_{30}), Sauter mean diameter (D_{32}), mean axial velocity, and mean **radial** velocity. The PDI system produces accurate measurements of D_{10} , D_{30} , D_{32} , and axial and radial velocity components. The uncertainty in the volume **flux** measurements was also found to be reasonable; however, on the average, the number density

measurements contain uncertainties greater than 50 %. The primary source of uncertainty in the volume flux and number density measurements is the difficulty accurately quantifying the probe area.

Phase Doppler interferometry permits accurate and non-intrusive characterization of fire sprinkler sprays. The major disadvantages of using PDI to characterize these sprays is the large coverage area of the spray compared with the small probe area of the PDI system, and the long data acquisition times due to the low number density of drops. Nonetheless, PDI appears to be the most accurate method of measuring mean drop sizes in residential fire sprinkler sprays. Future work will involve assessing the uncertainty of PDI measurements on the sprays produced by industrial fire sprinklers.

ACKNOWLEDGMENTS

The author would like to acknowledge Stefan Leigh for his assistance in determining the uncertainties in the reported measurements, and Cary Presser for the use of the PDI system. **Also**, the contributions of Jacob Goodman and Daniel Landau were invaluable in the data collection stage of this work.

REFERENCES

1. C. Yao and A. S. Kalelkar, Effect of Drop Size on Sprinkler Performance, *74th Annual Meeting of the National Fire Protection Association*, Toronto, pp. 254-268, 1970.
2. G. Grant, J. Brenton, and D. Drysdale, Fire Suppression by Water Sprays, *Prog. Energy Combust. Sci.*, vol. 26, pp. 79-130, 2000.
3. H. R. Baum, K. B. McGrattan, and R. G. Rehm, Three Dimensional Simulations of Fire Plume Dynamics, *J. Heat Transfer Soc. Japan*, vol. 35, pp. 45-52, 1997.
4. K. B. McGrattan, H. R. Baum, R. G. Rehm, Large Eddy Simulations of Smoke Movement, *Fire Safety J.*, vol 30, pp. 161-178, 1998.
5. J. R. Lawson, W. D. Walton, and D. D. Evans, Measurement of Droplet Size in Sprinkler Sprays, National Bureau of Standards, U. S. Department of Commerce, NBSIR 88-3715, Gaithersburg, MD, February 1988.
6. P. F. Nolan, Feasibility Study of Using Laser High Speed Cine Systems for the Characterization of Droplets from Sprinkler Sprays, The Swedish Fire Research Board, Stockholm, Sweden, 1989.
7. L. A. Jackman, P. F. Nolan, and H. P. Morgan, Characterization of Water Drops from Sprinkler Sprays, *Fire Suppression Research – First International Conference*, Stockholm, Sweden, pp. 159-184, 1992.
8. W. K. Chow and L. C. Shek, Physical Properties of a Sprinkler Water Spray, *Fire and Materials*, vol. 17, pp. 279-292, 1993.
9. H. Z. You, Sprinkler Drop-Size Measurement, Part II: An Investigation of the Spray Patterns of Selected Commercial Sprinklers with the FMRC PMS Droplet Measuring System, Technical Report 0G1e7.RA 070(A), Norwood, MA, May 1983.
10. H. Z. You, Investigation of Spray Patterns of Selected Sprinklers with the FMRC Drop Size Measuring System, *Fire Safety Science – Proceedings of the First International Symposium*, Gaithersburg, MD, pp. 1165-1176, October 1985.
11. T. S. Chan, Measurements of Water Density and Drop Size Distributions of Selected ESFR Sprinklers, *J. Fire Prot. Engr.*, vol. 6, pp. 79-87, 1994.
12. A. D. Putorti, T. D. Belsinger, and W. H. Twilley, Determination of Water Spray Drop Size and Speed from a Standard Orifice, Pendant Spray Sprinkler. Report of Test. National Institute of Standards and Technology, Gaithersburg, MD, May 1999.
13. D. T. Sheppard, P. D. Gandhi, and R. M. Lueptow, Predicting Sprinkler Water Distribution Using Particle Image Velocimetry. Research and Practice: Bridging the Gap. National Fire Protection Research Foundation, Orlando, FL, February 1999
14. P. D. Gandhi and D. Stepan, Using PDPA in Evaluation of Sprinklers, Proceedings Fire Suppression and Detection Research Application Symposium. Research and Practice: Bridging the Gap. National Fire Protection Research Foundation, Orlando, FL, pp. 65-78, February 1999.

15. R. A. Mugele and H. D. Evans, Droplet Size Distribution in Sprays, *Ind. Eng. Chem.*, vol. 43, no. 6, pp. 1317-1324, 1951.
16. B. N. Taylor and C. E. Kuyatt, Guidelines for Evaluating and Expressing the Uncertainty of NIST Measurement Results. NIST Technical Note 1297, National Institute of Standards and Technology, Gaithersburg, MD, September 1994.
17. American National Standard for Expressing Uncertainty – U.S. Guide to the Expression of Uncertainty in Measurement. ANSI/NCSL Report 2540-2-1997, National Conference of Standards Laboratories, Boulder, CO, October 1997.
18. J. Mandel, *Evaluation and Control of Measurements*, Marcel Dekker, New York, 1991.
19. J. A. Friedman and M. Renksizbulut, Investigating a Methanol Spray Flame Interacting with an Annular Air Jet using Phase Doppler Interferometry and Planar Laser-Induced Fluorescence. *Combustion and Flame*, vol. 117, pp. 661-684, 1999.
20. W. D. Bachalo and M. J. Houser, Development of the Phase/Doppler Spray Analyzer for Liquid Droplet Size and Velocity Characterizations. *AIAA/SAE/ASME 20th Joint Propulsion Conference*, Cincinnati, OH, June 1984.
21. W. D. Bachalo and M. J. Houser, Phase/Doppler Spray Analyzer for Simultaneous Measurements of Droplet Size and Velocity Distributions. *Opt. Eng.* vol. 1, pp. 583-590, 1984.
22. TSI Phase Doppler particle analyzer (PDPA) – operations manual. TSI Incorporated St. Paul, MN, 1999.
23. S. V. Sankar and W. D. Bachalo, Response Characteristics of the Phase-Doppler Particle Analyzer for Sizing Spherical Particles Larger than the Wavelength. *Appl. Opt.* vol. 30, pp. 1487-1496, 1991.
24. S. V. Sankar, W. D. Bachalo, and D. A. Robard, An Adaptive Intensity Validation Technique for Minimizing Trajectory Dependent Scattering Errors in Phase Doppler Interferometry. *4th International Congress on Optical Particle Sizing*. Nuremberg, Germany, March 1995.
25. J. Y. Zhu, R. C. Rudoff, E. J. Bachalo, and W. D. Bachalo, Number Density and Mass Flux Measurements using the Phase Doppler Particle Analyzer in Reacting and Non-reacting Swirling Flows. *AIAA 31st Aerospace Sciences Meeting & Exhibit*. Reno, Nevada, paper #AIAA-93-0361, 1993.
26. P. A. Strakey, D. G. Talley, S. V. Sankar, and W. D. Bachalo, The Use of Small Probe Volumes with Phase Doppler Interferometry. *ILASS-Americas 1998*. Sacramento, California, pp. 286-290, 1998.
27. H. Qui and C. T. Hsu, Method of Phase-Doppler Anemometry Free from the Measurement Volume Effect. *Appl. Opt.* vol. 38, pp. 2737-2742, 1999.
28. J. F. Widmann, C. Presser, and S. D. Leigh, Burst Splitting Events in Phase Doppler Interferometry Measurements. *Int. J. Multiphase Flow*, submitted, 2000.

29. A. Stuart and J. K. Ord, *Kendall's Advanced Theory of Statistics*, Fifth Edition of Volume 1 – Distribution Theory, Oxford University Press, New York, 1987.
30. B. J. Lazaro, Evaluation of Phase Doppler Particle Sizing in the Measurement of Optically Thick, High Number Density Sprays. United Technologies Research Center, East Hartford, Connecticut, Report UTRC9 1- 11, 1991.
31. T. Van Den Moortel, R. Santini, L. Tadriss, J. Pantaloni, Experimental Study of the Particle Flow in a Circulating Fluidized Bed using a Phase Doppler Particle Analyzer: A New Post-processing Data Algorithm. *Int. J. Multiphase Flow*. vol. **23**, pp. 1189-1209, 1997.
32. J. F. Widmann, C. Presser, and S. D. Leigh, Improving Phase Doppler Volume Flux Measurements in Low Data Rate Applications. *Meas. Sci. Technol.* submitted, **2000**.
33. C. Fandrey, A. Naqwi, J. Shakal, and H. Zhang, A Phase Doppler System for High-Concentration Sprays. *10th International Symposium on Applications of Laser Techniques to Fluid Mechanics*. Lisbon, Portugal, July 2000.

MEASUREMENT	TYPE B UNCERTAINTY
Size (individual drops)	
Scattering angle	1 %
Refractive index	1 %
Detector spacing	Negligible
Combined Type B for Size	1.4 %
Velocity (individual drops)	
Frequency measurement	25 %
Fringe spacing	Negligible
Combined Type B for Velocity	25 %
Arithmetic mean diameter, D_{10}	
Missed drops	2 %
Saturated signals	Negligible
Trajectory ambiguity errors	Negligible
Invalidated drops	1 %
Diameter vs. phase shift curve	Negligible
Probe volume correction	0.5 %
Combined Type B for D_{10}	2.3 %
Volume mean diameter, D_{30}	
Missed drops	Negligible
Saturated signals	Negligible
Trajectory ambiguity errors	0.5 %
Invalidated drops	1 %
Diameter vs. phase shift curve	Negligible
Probe volume correction	0.33 %
Combined Type B for D_{30}	1.2 %
Sauter mean diameter, D_{32}	
Missed drops	Negligible
Saturated signals	Negligible
Trajectory ambiguity errors	0.5 %
Invalidated drops	1 %
Diameter vs. phase shift curve	Negligible
Probe volume correction	0.2 %
Combined Type B for D_{32}	1.1 %
Mean Velocity	
Frequency measurement	3 %
Invalidated drops	Negligible
Missed drops	Negligible
Combined Type B for Mean Velocity	3 %
Volume Flux	14.0 %
Number Density	21 %
Probe Area	15 %

Table 2. Mean relative uncertainties, $2U_c$, in the PDI measurements.

MEASUREMENT	COMBINED STANDARD UNCERTAINTY, $k = 2$
Arithmetic Mean Diameter, D_{10}	6.4 %
Volume Mean Diameter, D_{30}	4.1 %
Sauter Mean Diameter, D_{32}	3.6 %
Mean Axial Velocity, v_z	6.9 %
Mean Radial Velocity, v_r	8.4 %
Volume Flux, F	30.2 %
Number Density, N_d	54.1 %

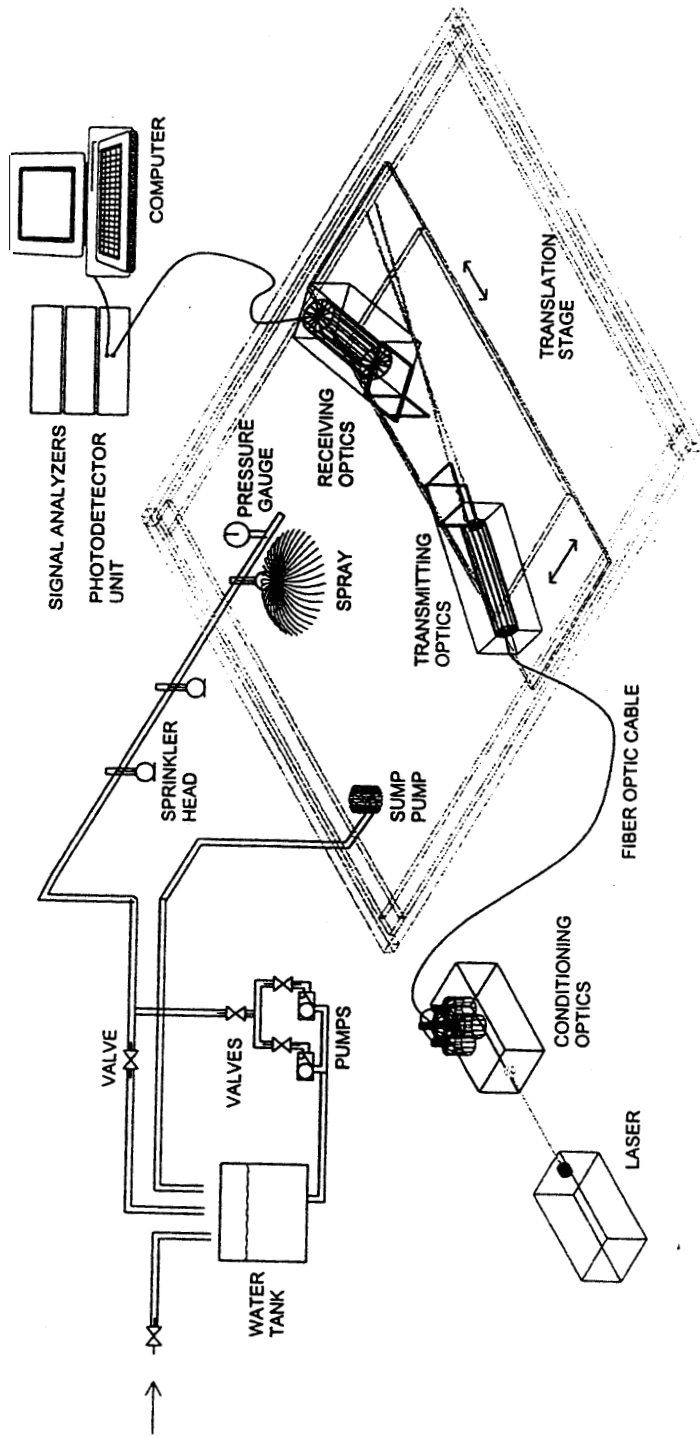
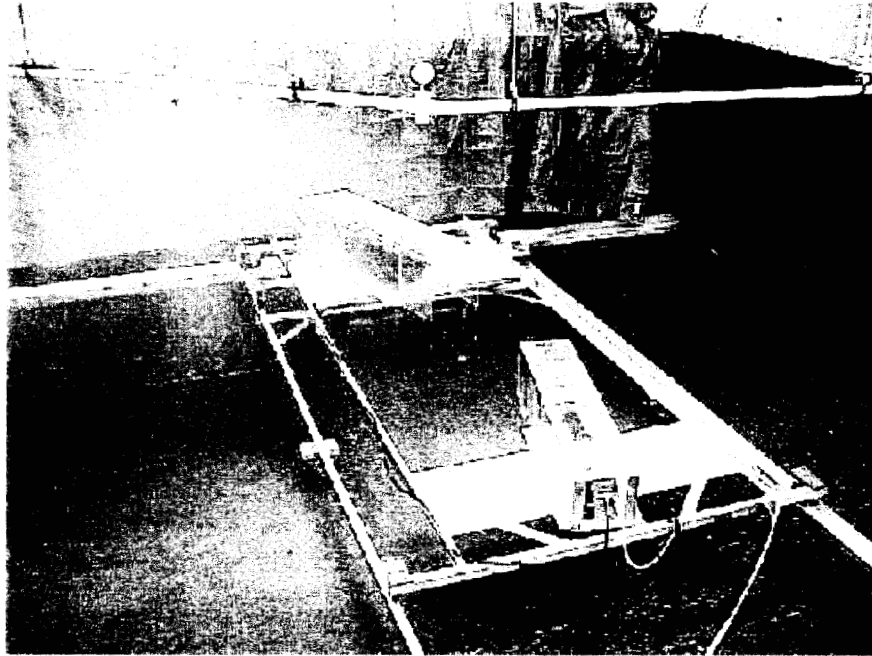


Fig. 1 Schematic of the experimental facility.

A



B

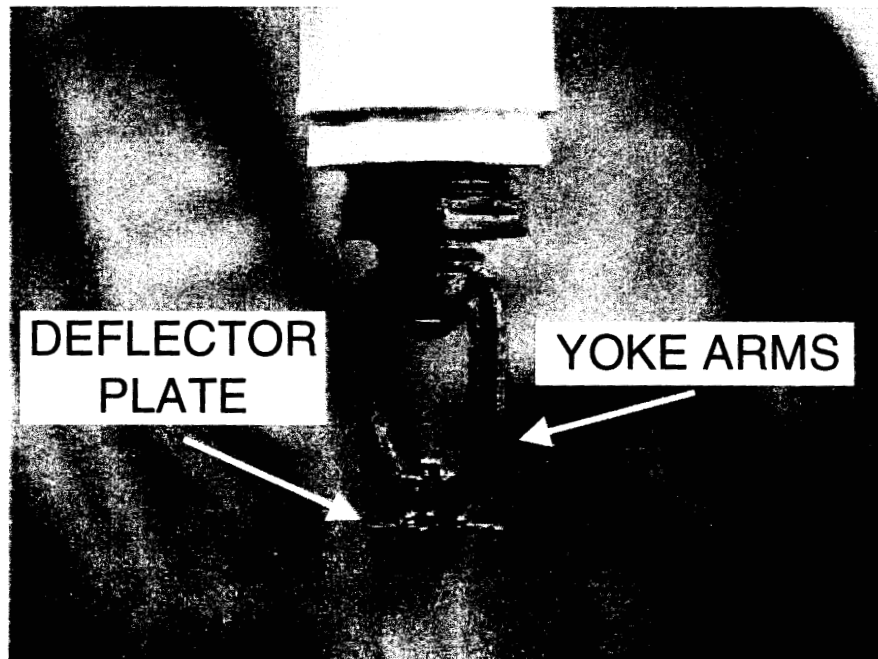


Fig. 2 Photograph of the (A) experimental facility and the (B) residential sprinkler used in this study.

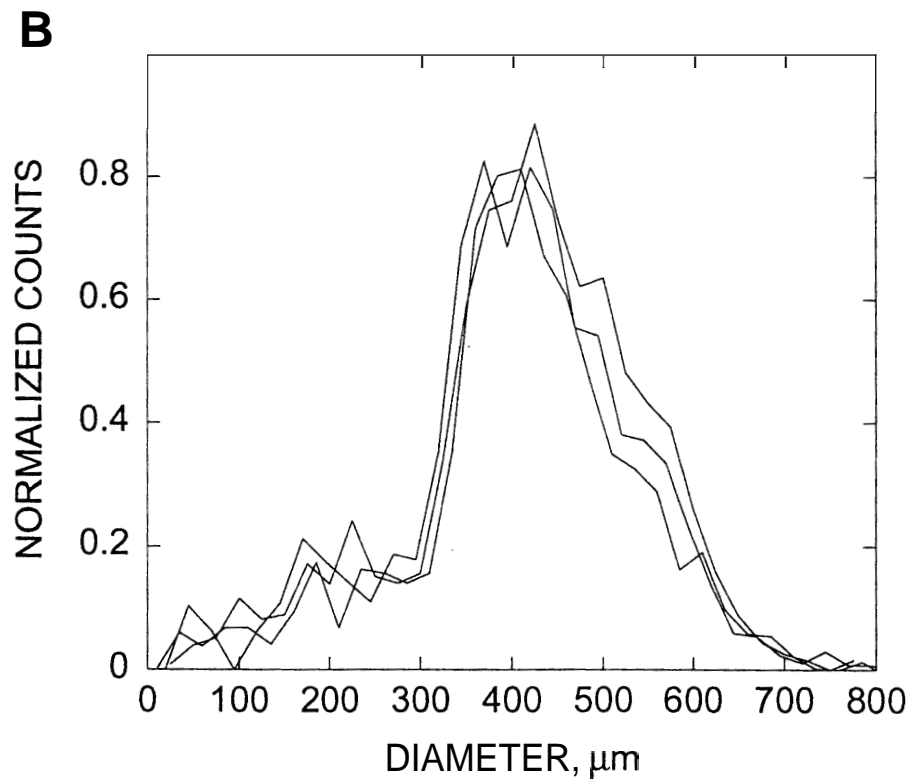
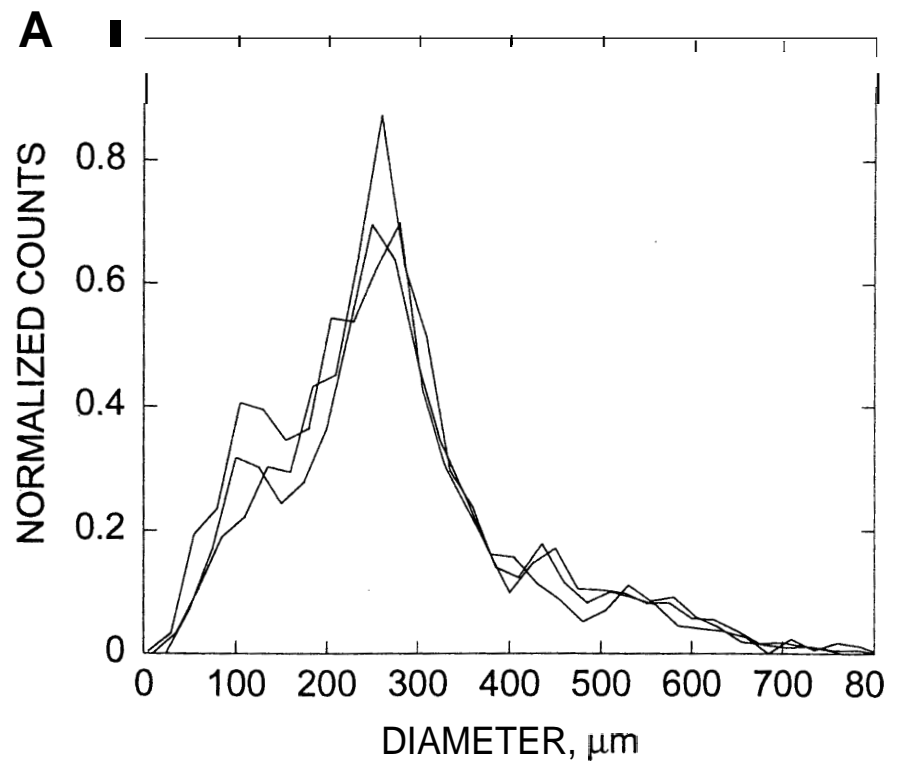


Fig. 3 Representative size distributions obtained with the PDI system at locations (A) near and (B) far from the fire sprinkler axis.

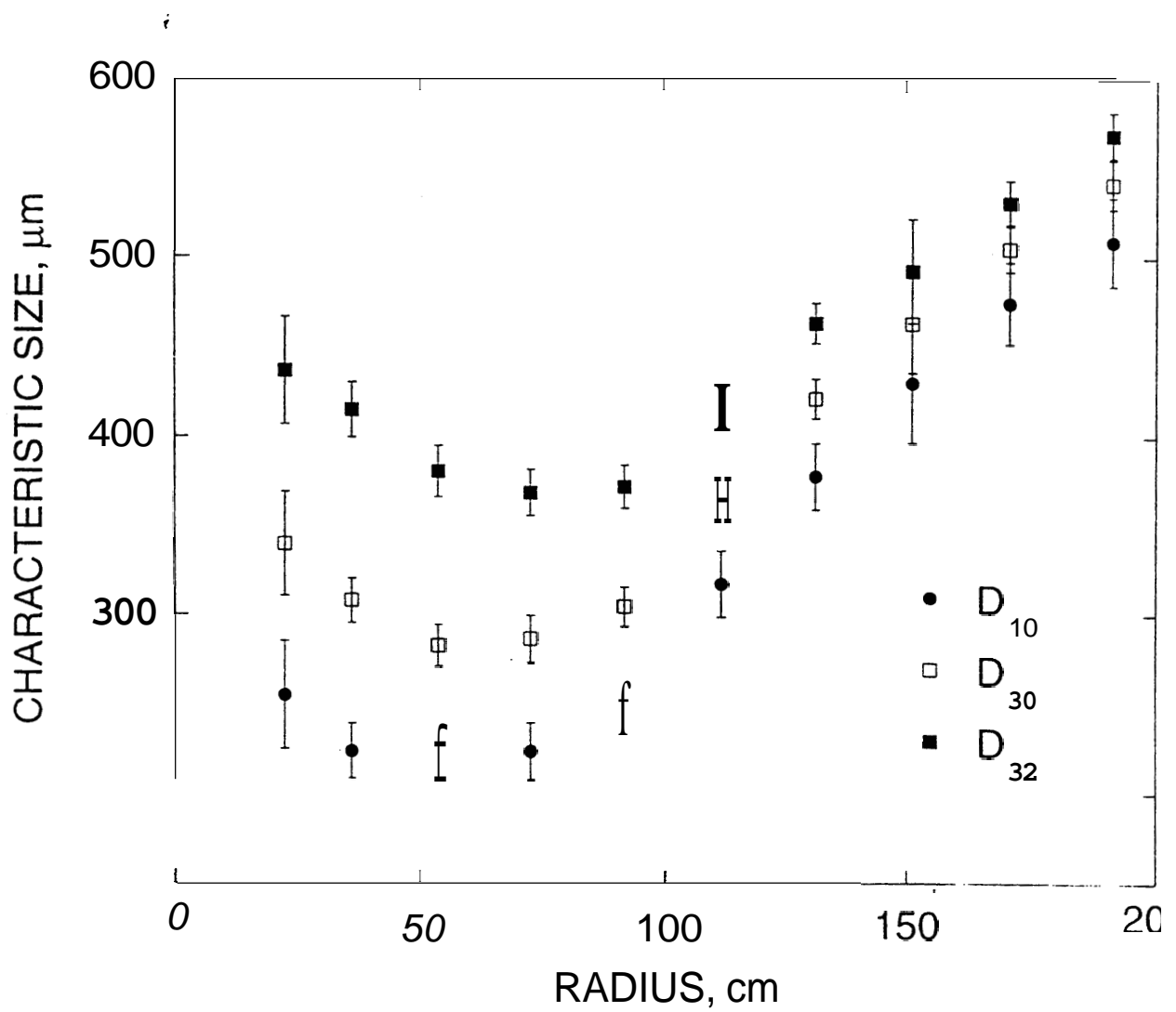


Fig. 4 The arithmetic mean diameter (D_{10}), volume mean diameter (D_{30}), and Sauter mean diameter (D_{32}) as a function of the radial coordinate in the spray.

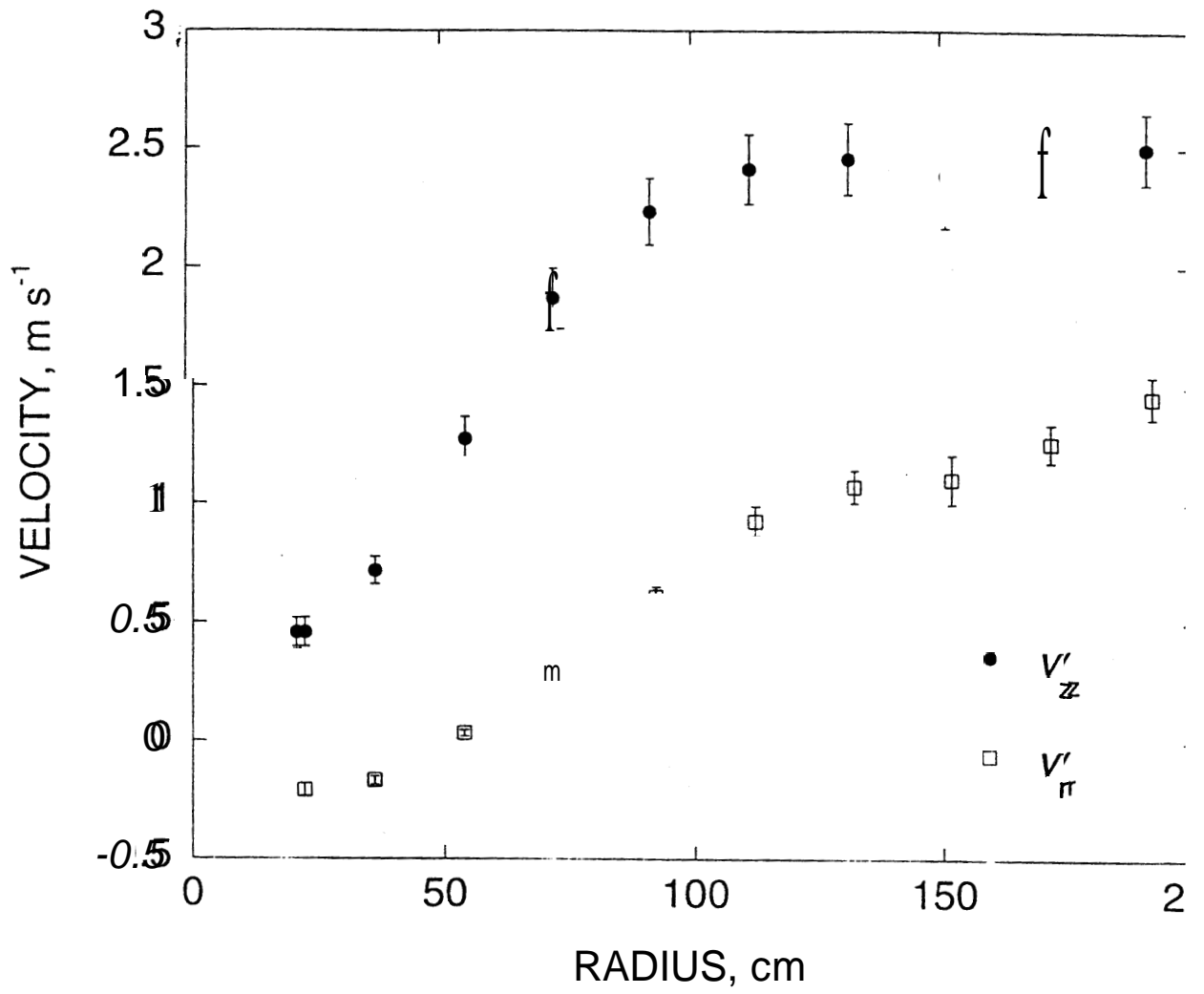


Fig. 5 The mean axial and radial drop velocities measured in the spray as a function of the radial coordinate.

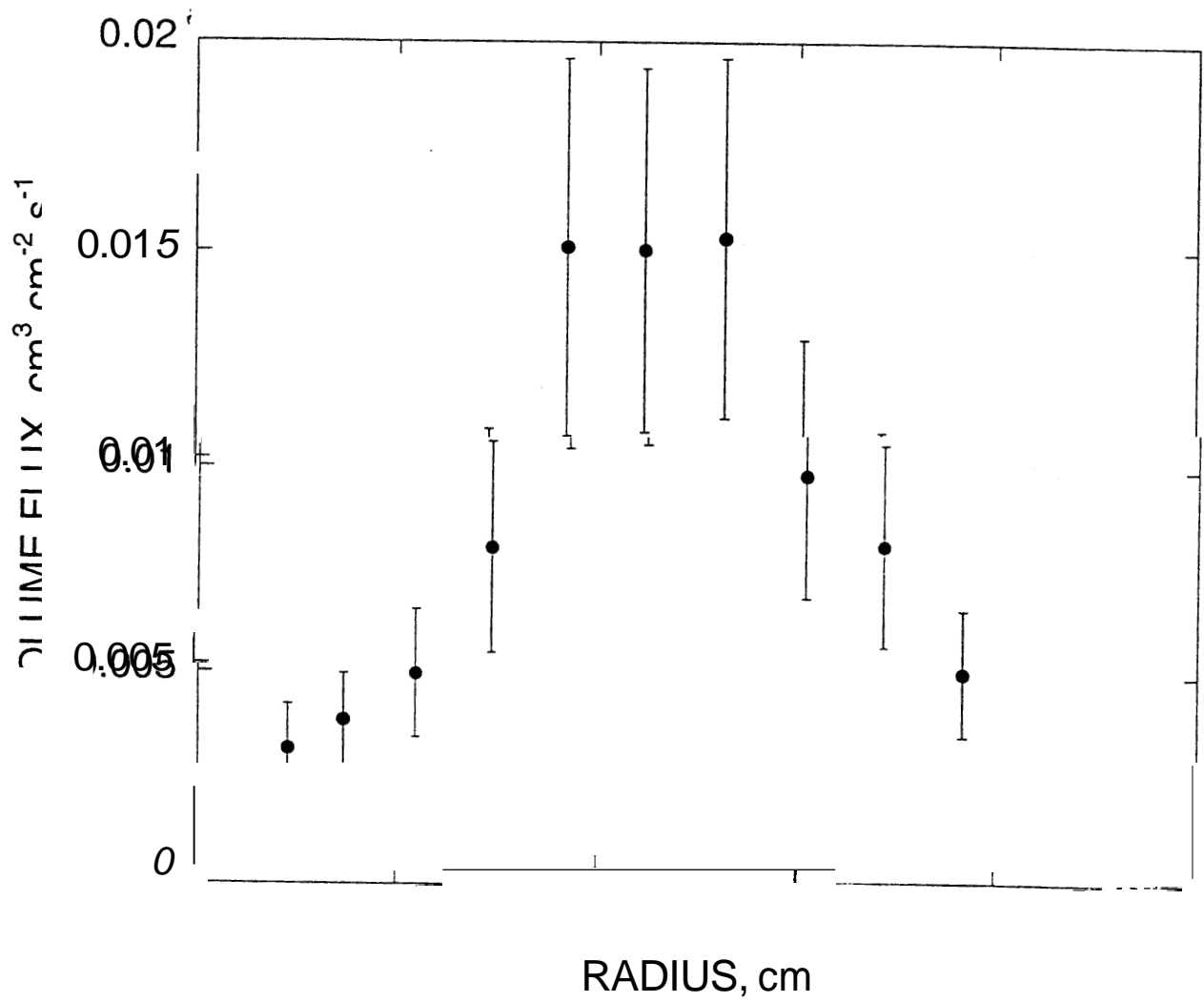


Fig. 6 The volume **flux** measured with the PDI system as a function of the radial coordinate.

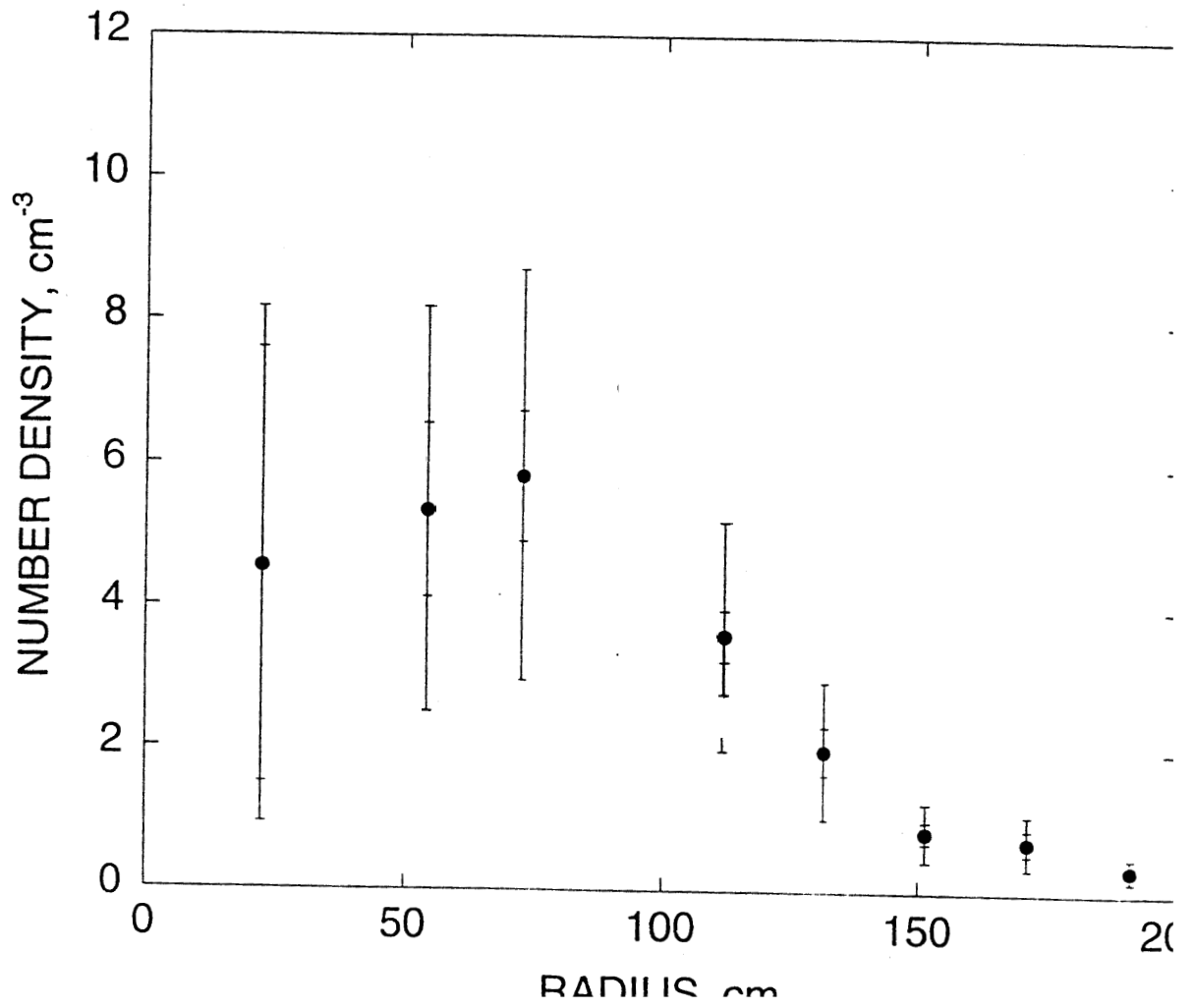


Fig. 7 The measured number density as a function of the radial coordinate.

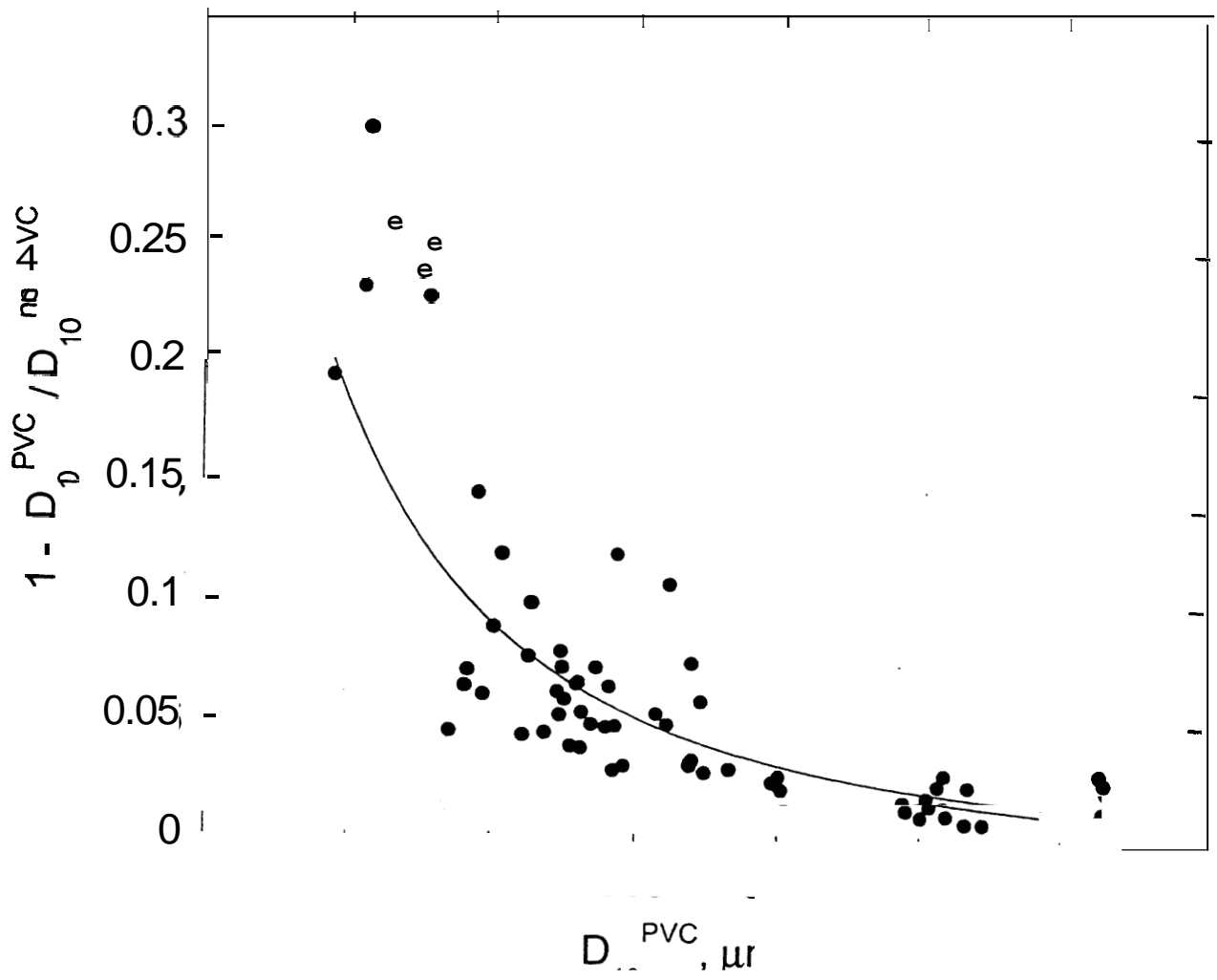


Fig. 8 The effect of the probe volume correction on the arithmetic mean diameter, D_{10} .

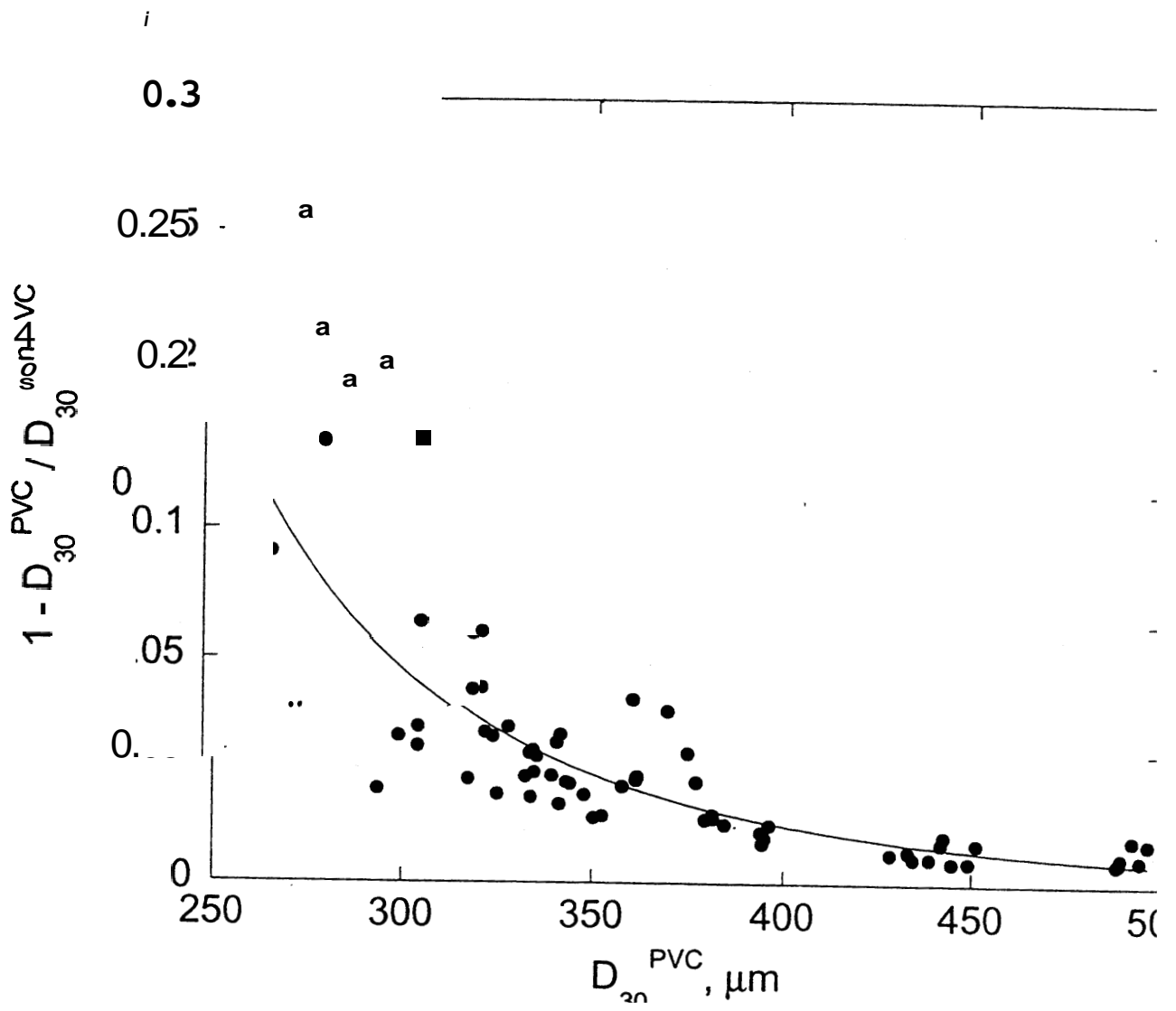


Fig. 9 The effect of the probe volume correction on the volume mean diameter, D_{30} .

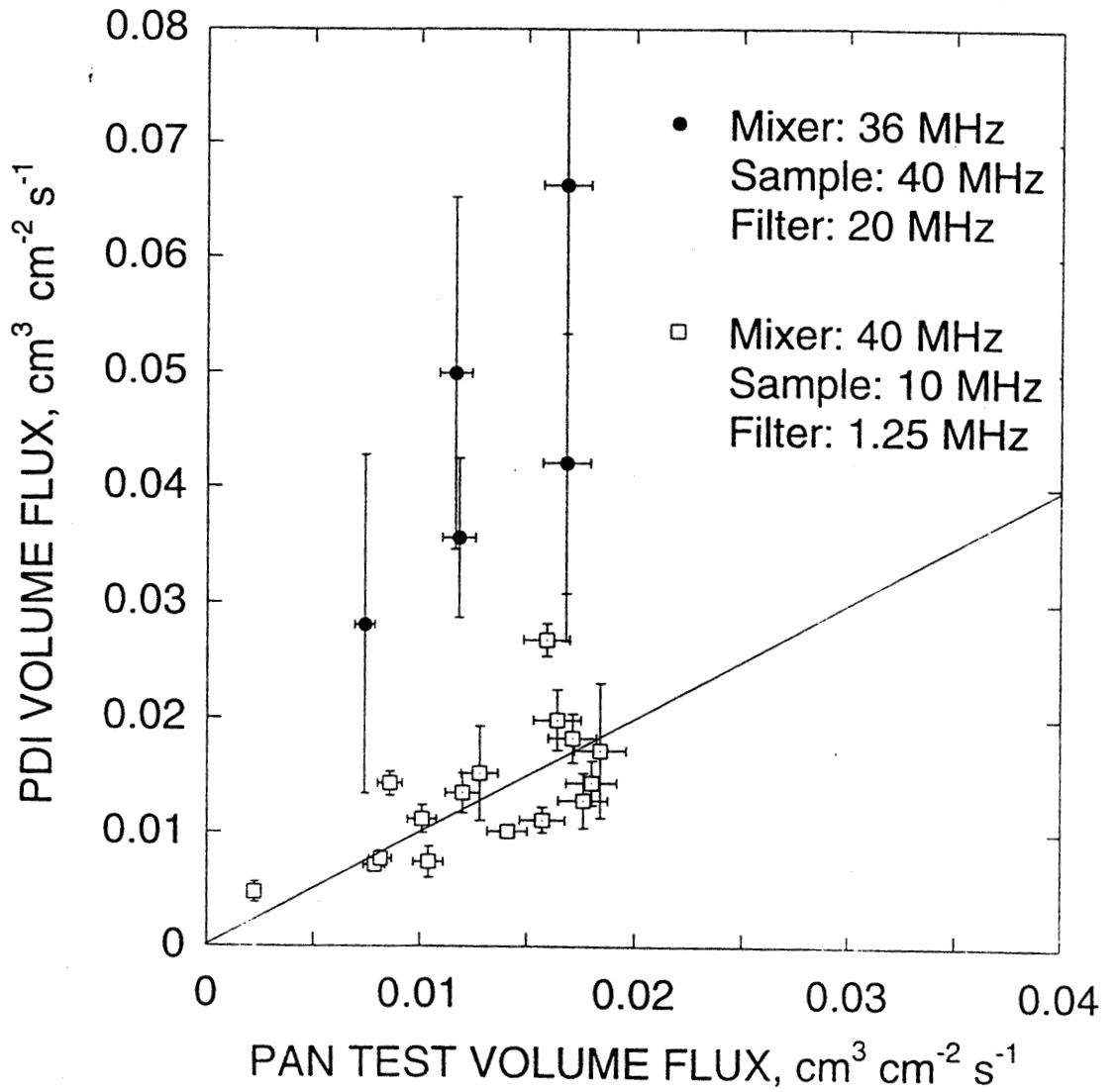


Fig. 11 Comparison of the volume flux measured with the PDI system and the pan test measurements.

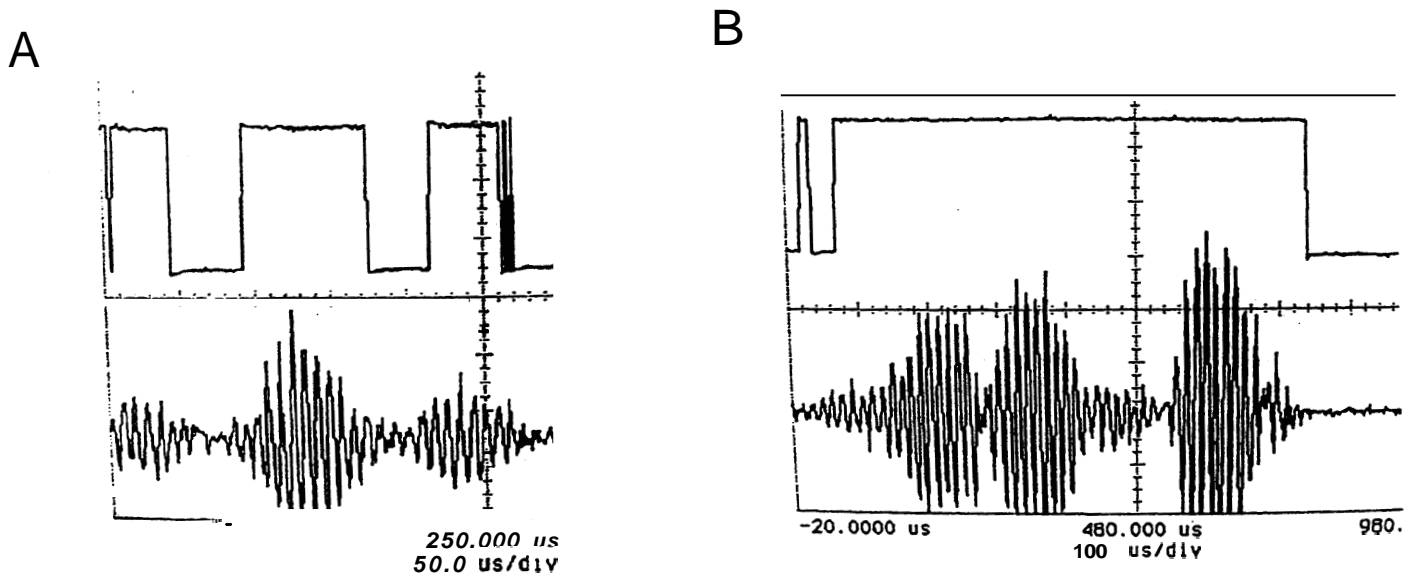


Fig. 12 Oscilloscope traces showing the effect of burst splitting on the gate signal and the Doppler signal. The operating conditions correspond to (A) mixer frequency = **36 MHz**, sample frequency = **40 MHz**, and low pass filter = **20 MHz**, and (B) mixer frequency = **40 MHz**, sample frequency = **10 MHz**, and low pass filter = **1.25 MHz**.

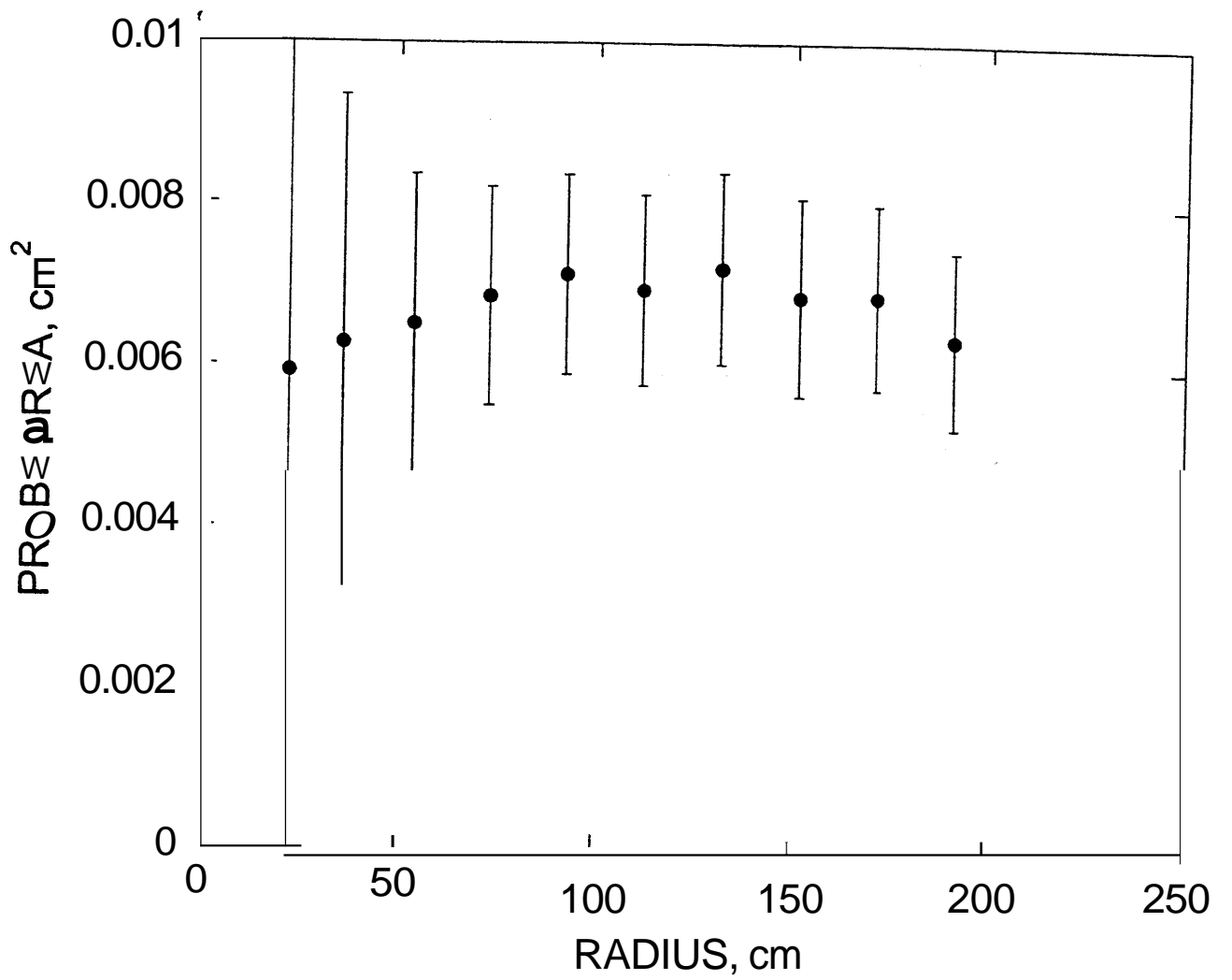


Fig. 13 The measured probe area as a function of the radial coordinate.